

Electronic Supplementary Information (ESI) to:

# Nitroxide Radical Surfactants Enable Electrocatalytic Oxidation of Fatty Alcohols in Water

*Chanaka J. Mudugamuwa,<sup>a</sup> Yuan Xie,<sup>a</sup> Kai Zhang,<sup>b</sup> Thomas P. Nicholls,<sup>a</sup> Justin M. Chalker,<sup>a</sup>  
and Zhongfan Jia<sup>a\*</sup>*

a. Institute for Nanoscale Science and Technology, College of Science and Engineering,  
Flinders University, Bedford Park, South Australia 5042, Australia.

b. Key Laboratory of Surface & Interface Science of Polymer Materials of Zhejiang  
Province, Department of Chemistry, Zhejiang Sci-Tech University, 928 Second Street,  
Hangzhou 310018, China.

To whom all correspondence should be addressed. E-mail: [zhongfan.jia@flinders.edu.au](mailto:zhongfan.jia@flinders.edu.au) (ZJ).

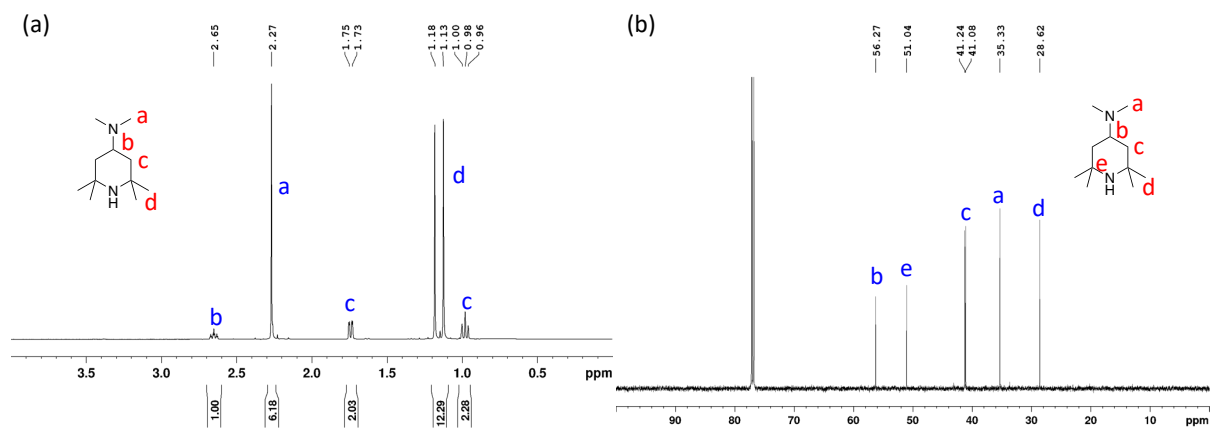


**Figure S1.**  $^1\text{H}$  (a) and  $^{13}\text{C}$  (b) NMR spectra of 4-dimethylamino-2,2,6,6-tetramethylpiperidine (DMTMP) in  $\text{CDCl}_3$ .

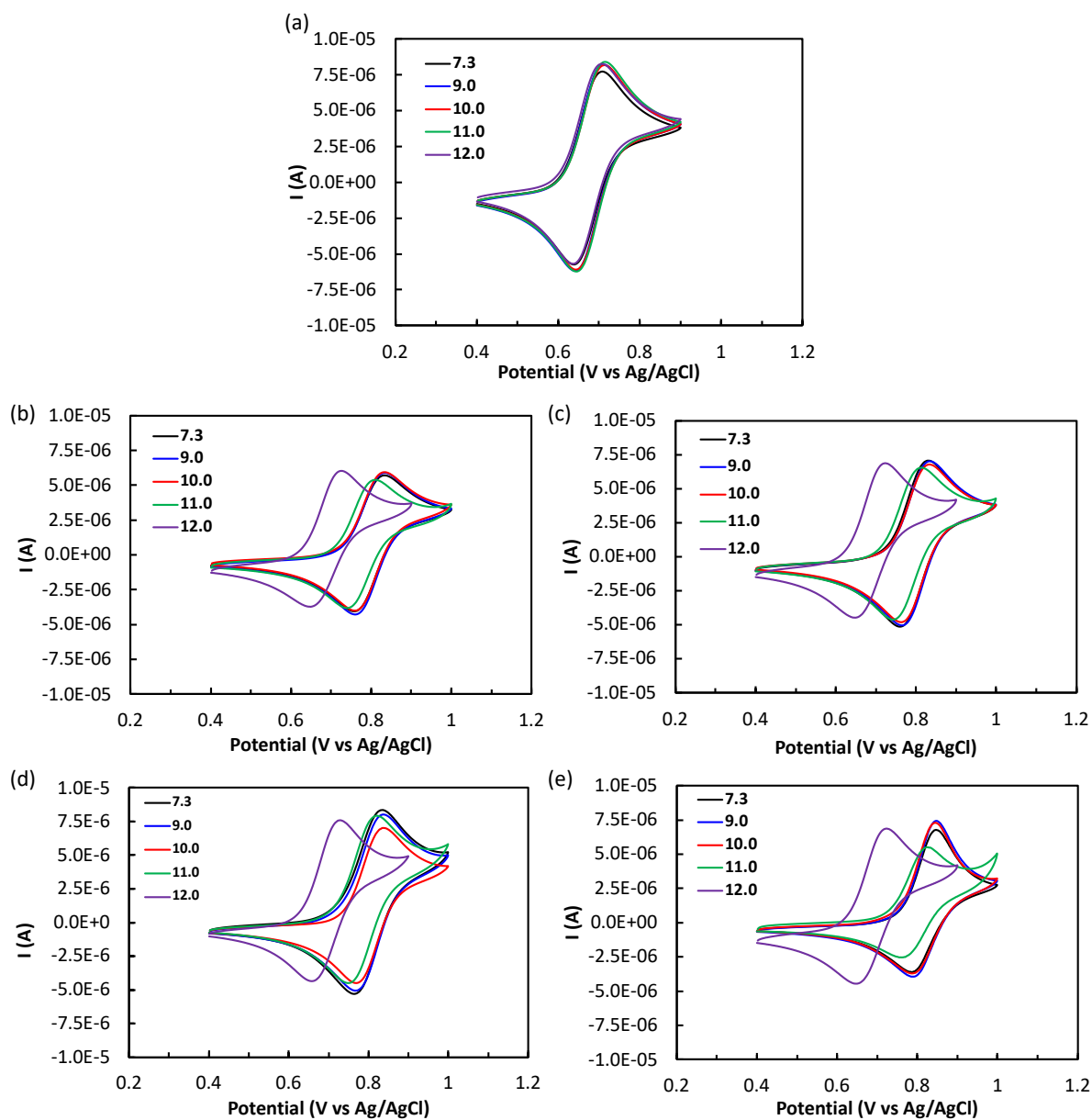


**Figure S2.** CVs of ACT (a) and TEMPO surfactants with C4 (b), C8 (c), C10 (d), and C14 (e) alkyl chains in different pH buffer solutions. Solution condition: PBS buffer 7.3 and carbonate buffer 9.0. to 12.0 0.1 M with 0.1 M NaCl, TEMPO radicals, 1 mM. Glassy carbon electrode with a scan rate of 50 mV/s.

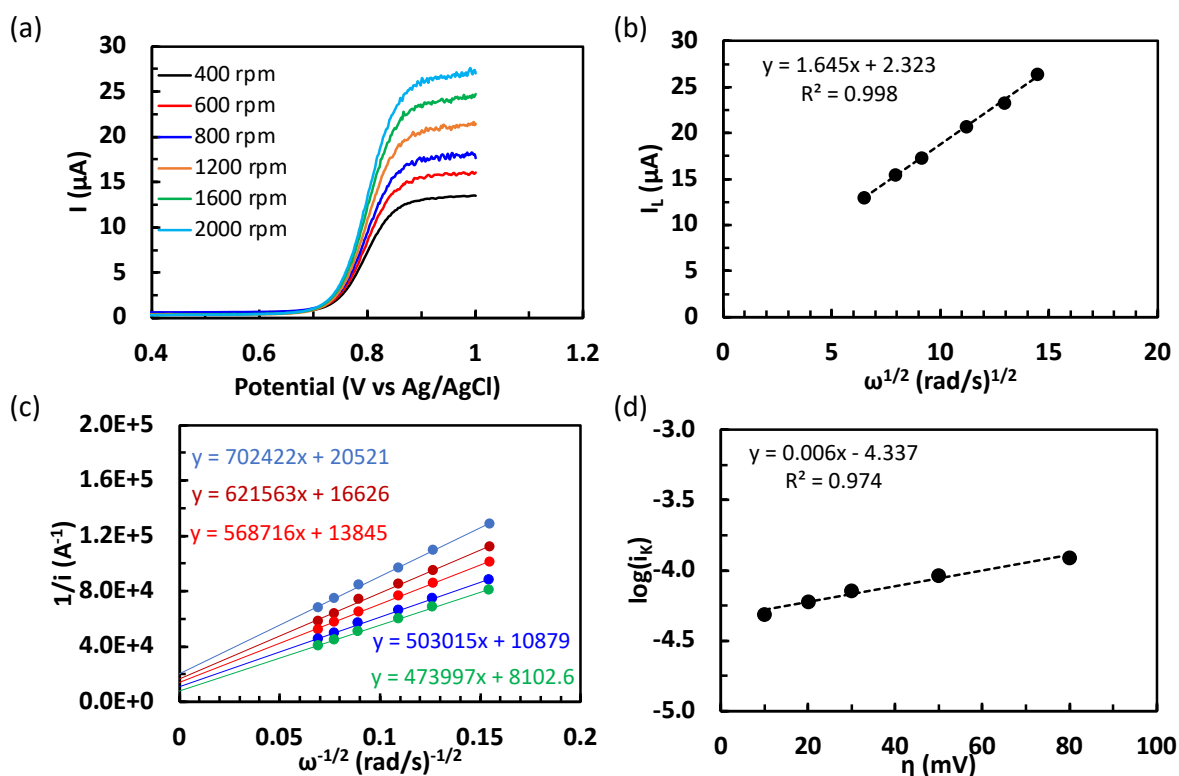


**Figure S3.** Typical RDE measurements of C8-NO· in a pH 7.3 buffer with 0.1 M NaCl and analysis. (a) Linear scan voltammograms of C8-NO· (1.0 mM) at 10 mV/s at various rotation speeds from 400 rpm to 2000 rpm. (b) The Levich plot of limiting currents (adopted at 0.9 V vs Ag/AgCl) vs the square roots of rotation rates. (c) The Koutecký-Levich plot for different overpotentials ( $\eta$ ) to obtain the kinetic current  $i_k$  (when  $\omega^{-1/2}$  approaching zero). (d) The Tafel plot of kinetic currents  $i_k$  vs overpotentials  $\eta$  to obtain the heterogeneous electron transfer rate constant  $k_0$ .

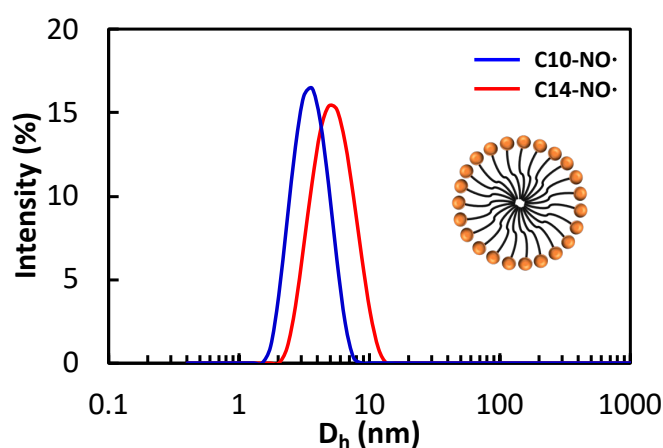


**Figure S4.** DLS of C10-NO· at 20 mg/mL and C14-NO· at 10 mg/mL in 0.1 M pH 10 buffer with 0.1 M NaCl.

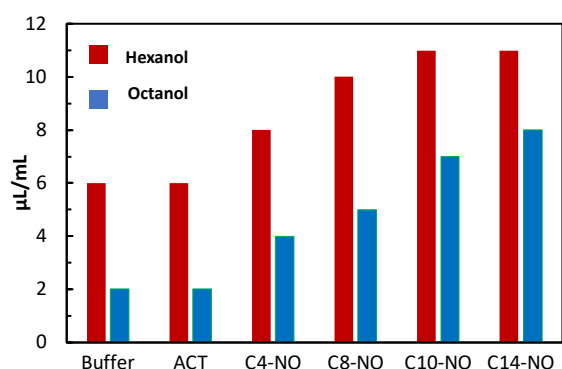


**Figure S5.** Solubility of hexanol and octanol in buffer 10.0 in the absence or presence of ACT or TEMPO surfactant 1mM.

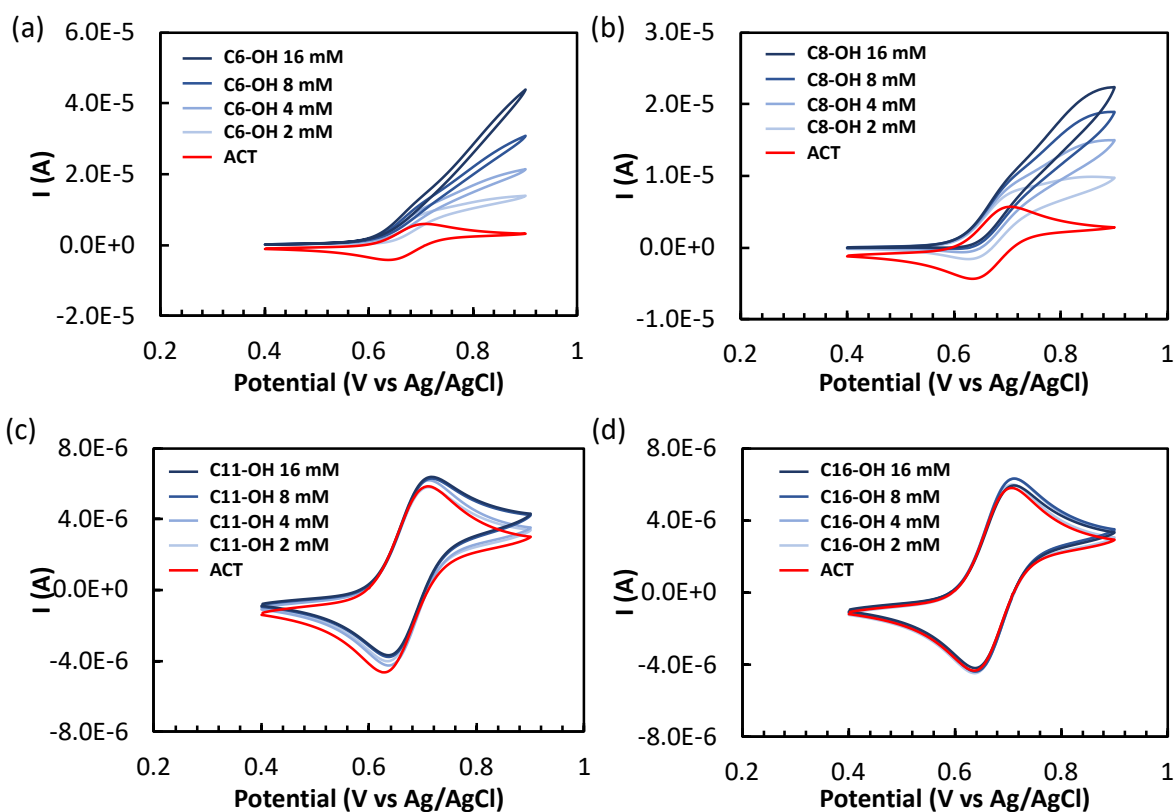


**Figure S6.** CVs of ACT-mediated electrocatalytic oxidation of (a) C6-OH, (b) C8-OH (c) C11-OH and (d) C16-OH at different alcohol concentrations. Solution conditions: ACT 1 mM, pH 10 buffer  $\text{Na}_2\text{CO}_3/\text{NaHCO}_3$  0.1 M with NaCl 0.1 M, GC working electrode and Ag/AgCl reference electrode, scan rate was 25 mV/s.

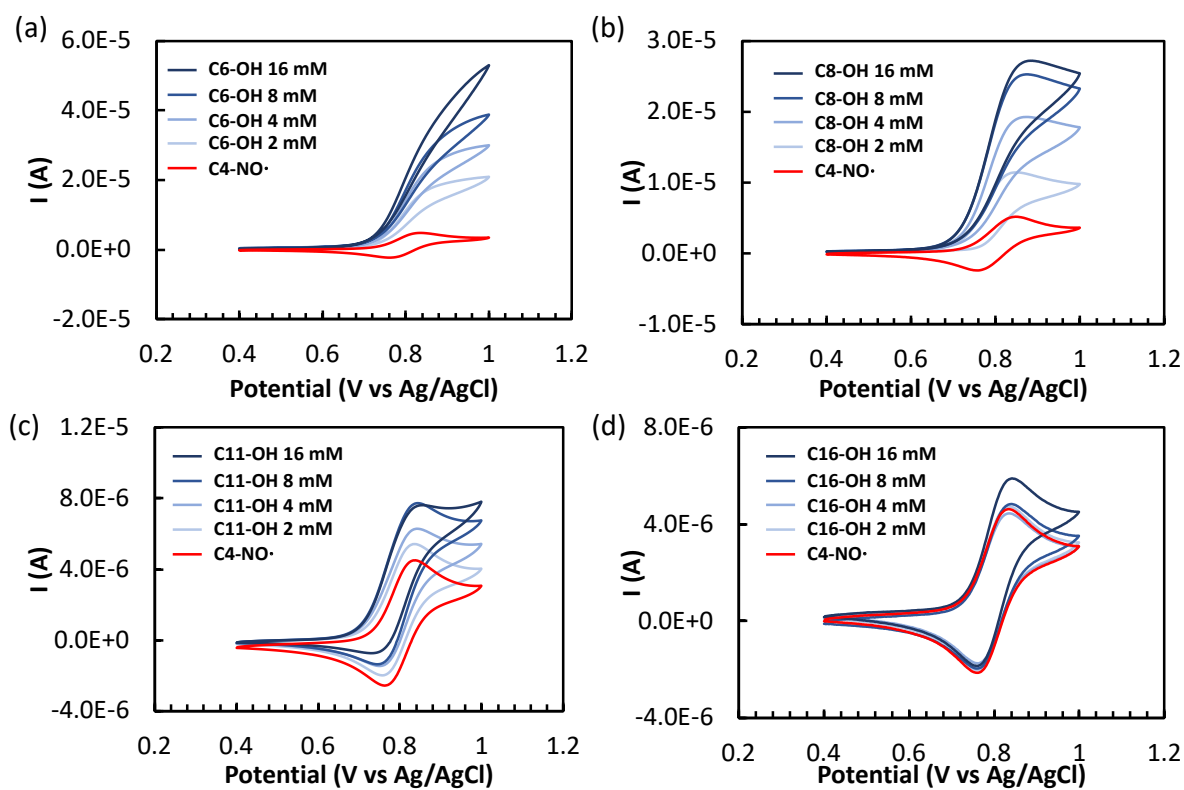


**Figure S7.** CVs of C4-NO $\cdot$  electrocatalytic oxidation of (a) C6-OH, (b) C8-OH (c) C11-OH and (d) C16-OH at different alcohol concentrations. Solution conditions: C4-NO $\cdot$  1 mM, pH 10 buffer Na<sub>2</sub>CO<sub>3</sub>/NaHCO<sub>3</sub> 0.1 M with NaCl 0.1 M, GC working electrode and Ag/AgCl reference electrode, scan rate was 25 mV/s.

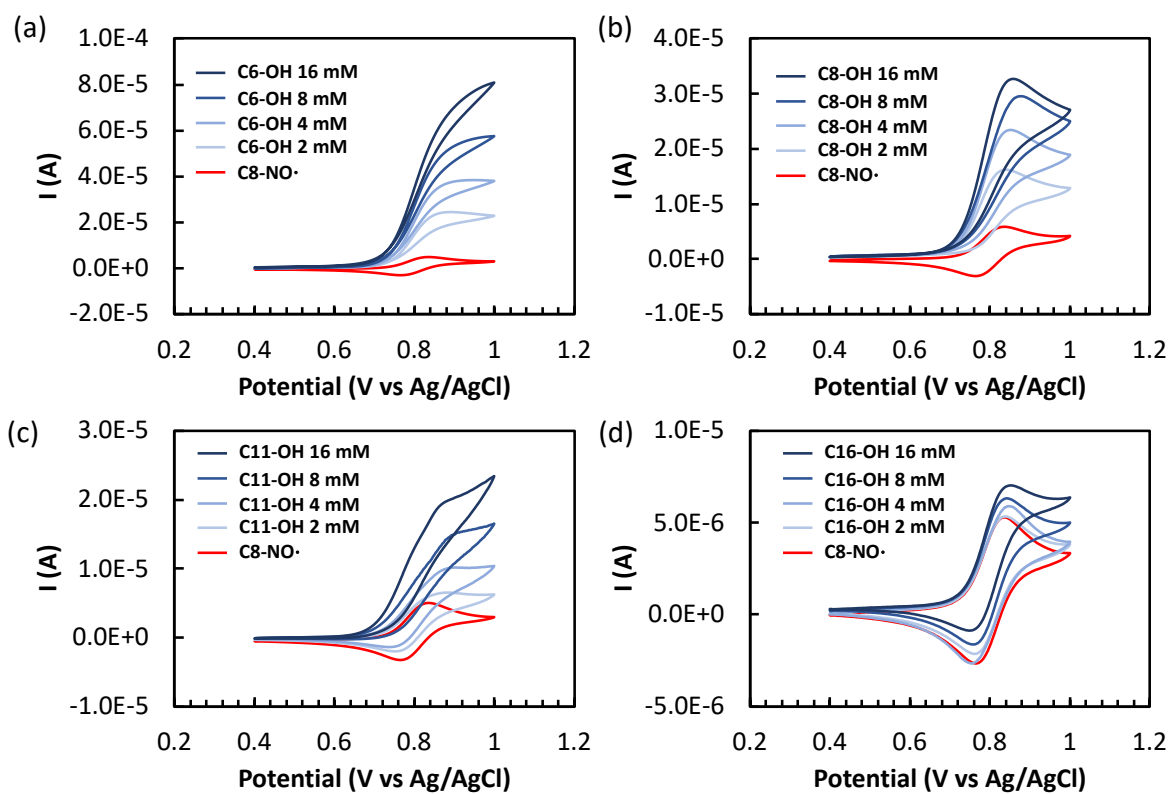


**Figure S8.** CVs of C8-NO· electrocatalytic oxidation of (a) C6-OH, (b) C8-OH (c) C11-OH and (d) C16-OH at different alcohol concentrations. Solution conditions: C8-NO· 1 mM, pH 10 buffer  $\text{Na}_2\text{CO}_3/\text{NaHCO}_3$  0.1 M with NaCl 0.1 M, GC working electrode and Ag/AgCl reference electrode, scan rate was 25 mV/s.

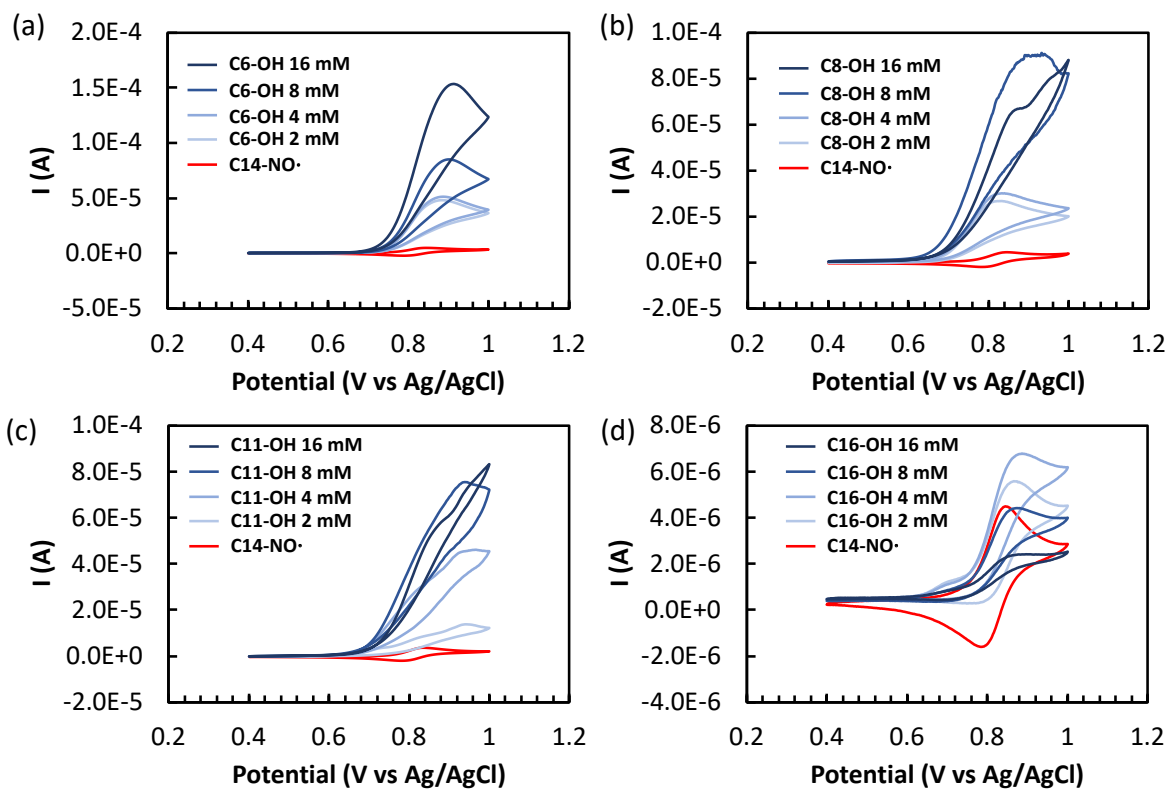


**Figure S9.** CVs of C14-NO• electrocatalytic oxidation of (a) C6-OH, (b) C8-OH (c) C11-OH and (d) C16-OH at different alcohol concentrations. Solution conditions: C14-NO• 1 mM, pH 10 buffer Na<sub>2</sub>CO<sub>3</sub>/NaHCO<sub>3</sub> 0.1 M with NaCl 0.1 M, GC working electrode and Ag/AgCl reference electrode, scan rate was 25 mV/s.

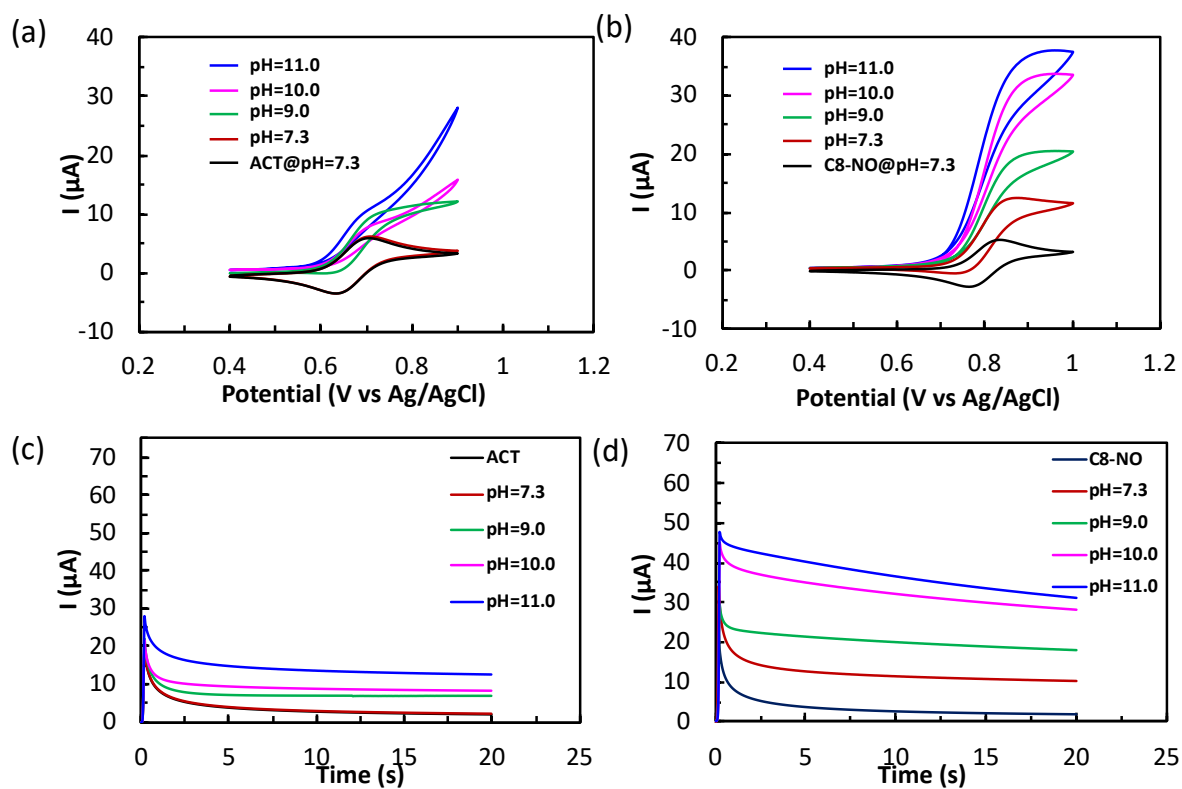


**Figure S10:** pH-dependent catalytic oxidation of C6-OH by (a, c) ACT and (b, d) C8-NO $\cdot$ , (a) and (b) were CVs and (c) and (d) were CAs. Solution conditions: catalyst 1 mM, GC working electrode and Ag/AgCl reference electrode; scan rates for all CVs were 25 mV/s. The applied potentials for CA were 0.8 V for ACT and 0.9 V for C8-NO $\cdot$ .

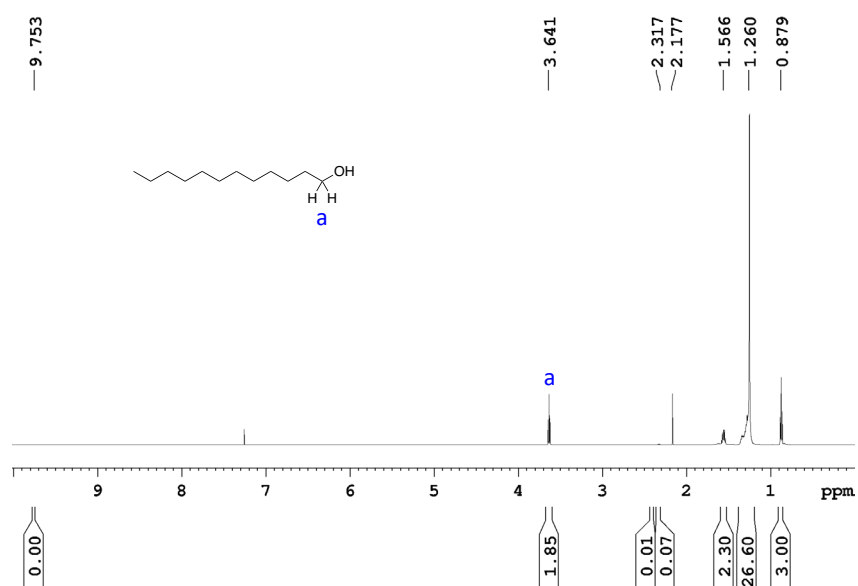


**Figure S11.**  $^1\text{H}$  NMR of the crude product oxidized from C12-OH (20 mM) by ACT (1 mM) in pH 10 buffer. Applied potential 0.8 V vs Ag/AgCl. Carbon felt  $20\text{ cm}^2$  as the working electrode, Pt wire 16 cm as the counter electrode, Ag/AgCl as the reference electrode, and temperature  $35\text{ }^\circ\text{C}$ .

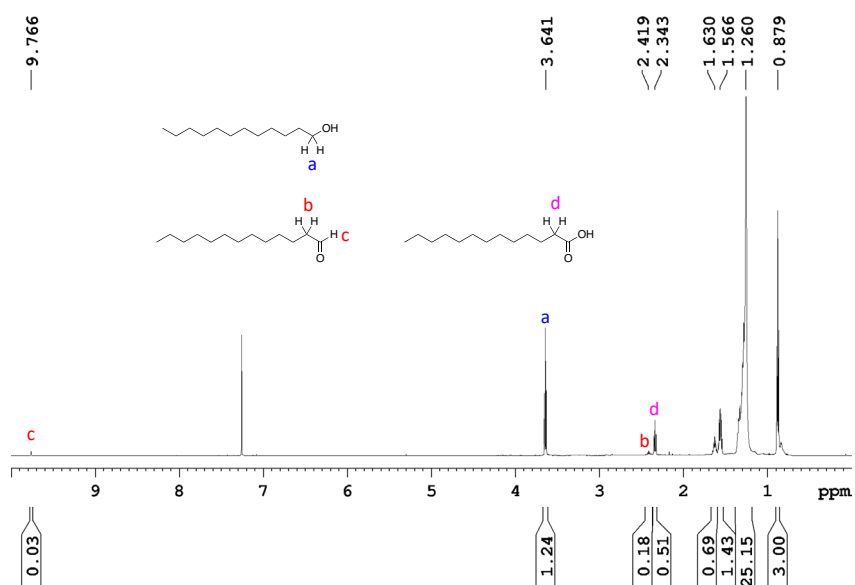


**Figure S12.**  $^1\text{H}$  NMR of the crude product oxidized from C12-OH (20 mM) by C10-NO $\cdot$  (1 mM) in pH 10 buffer. Applied potential 0.9 V vs Ag/AgCl. Carbon felt  $20\text{ cm}^2$  as the working electrode, Pt wire 16 cm as the counter electrode, Ag/AgCl as the reference electrode, and temperature  $35\text{ }^\circ\text{C}$ .

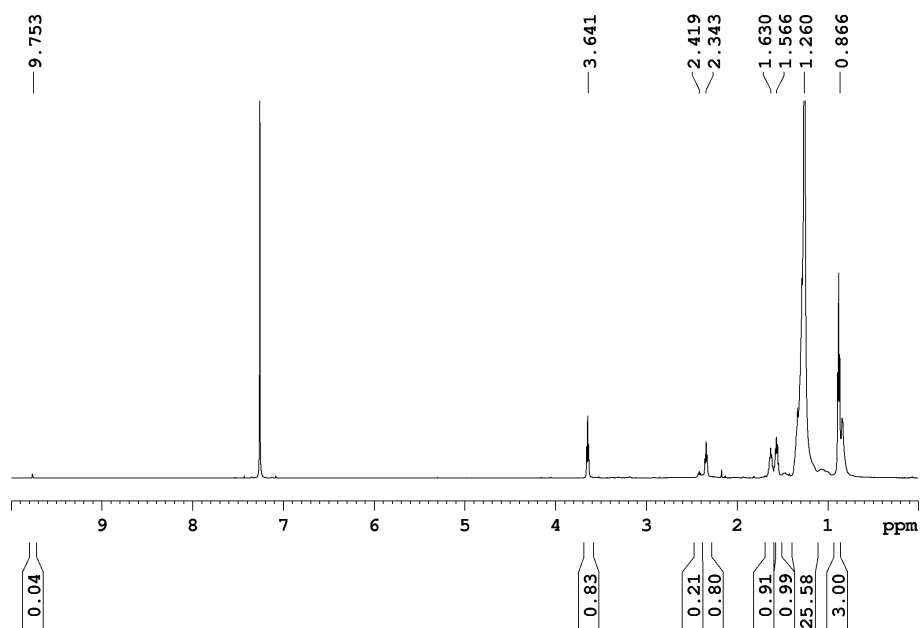


**Figure S13.**  $^1\text{H}$  NMR of the crude product oxidized from C12-OH (20 mM) by C14-NO $\cdot$  (1 mM) in pH 10 buffer. Applied potential 0.9 V vs Ag/AgCl. Carbon felt 20 cm $^2$  as the working electrode, Pt wire 16 cm as the counter electrode, Ag/AgCl as the reference electrode, and temperature 35  $^\circ\text{C}$ .

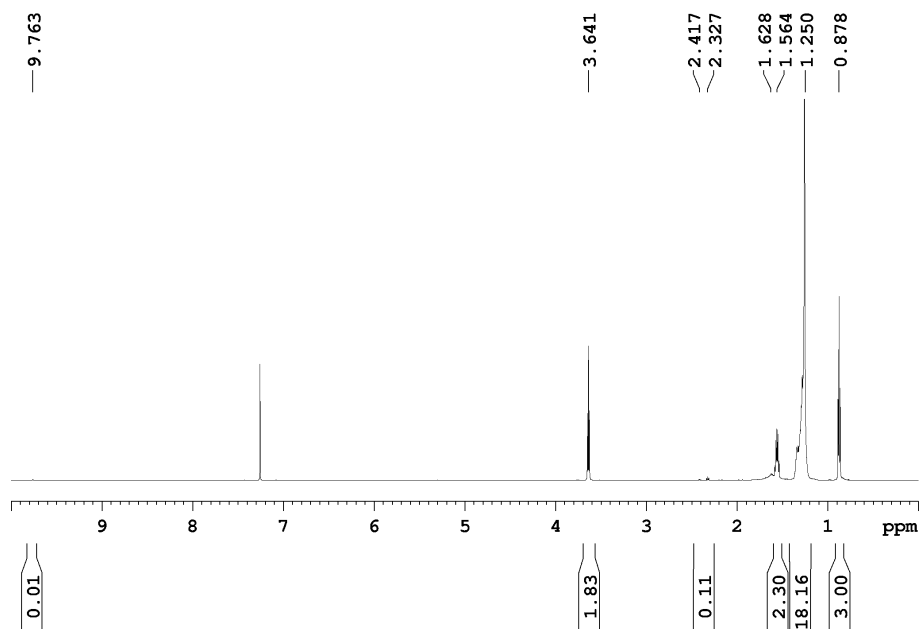


**Figure S14.**  $^1\text{H}$  NMR of the crude product oxidized from C16-OH (20 mM) by ACT (1 mM) in pH 10 buffer. Applied potential 0.9 V vs Ag/AgCl. Carbon felt 20 cm $^2$  as the working electrode, Pt wire 16 cm as the counter electrode, Ag/AgCl as the reference electrode, and temperature 60  $^\circ\text{C}$ .

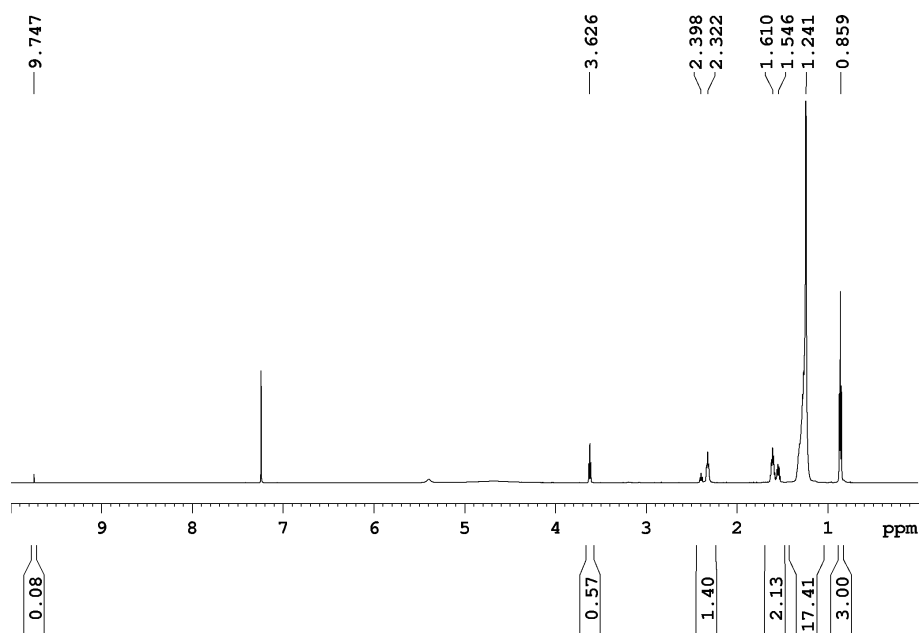


**Figure S15.**  $^1\text{H}$  NMR of the crude product oxidized from C16-OH (20 mM) by C10-NO $\cdot$  (1 mM) in pH 10 buffer. Applied potential 0.9 V vs Ag/AgCl. Carbon felt 20 cm $^2$  as the working electrode, Pt wire 16 cm as the counter electrode, Ag/AgCl as the reference electrode, and temperature 60  $^\circ\text{C}$ .

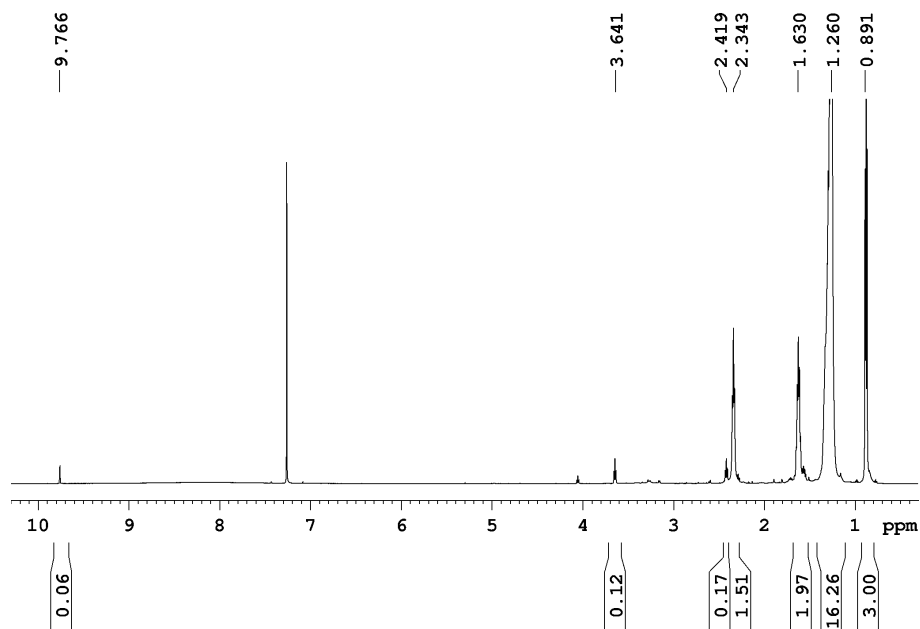


**Figure S16.**  $^1\text{H}$  NMR of the crude product oxidized from C16-OH (20 mM) by C14-NO $\cdot$  (1 mM) in pH 10 buffer. Applied potential 0.9 V vs Ag/AgCl. Carbon felt 20 cm $^2$  as the working electrode, Pt wire 16 cm as the counter electrode, Ag/AgCl as the reference electrode, and temperature 60  $^\circ\text{C}$ .

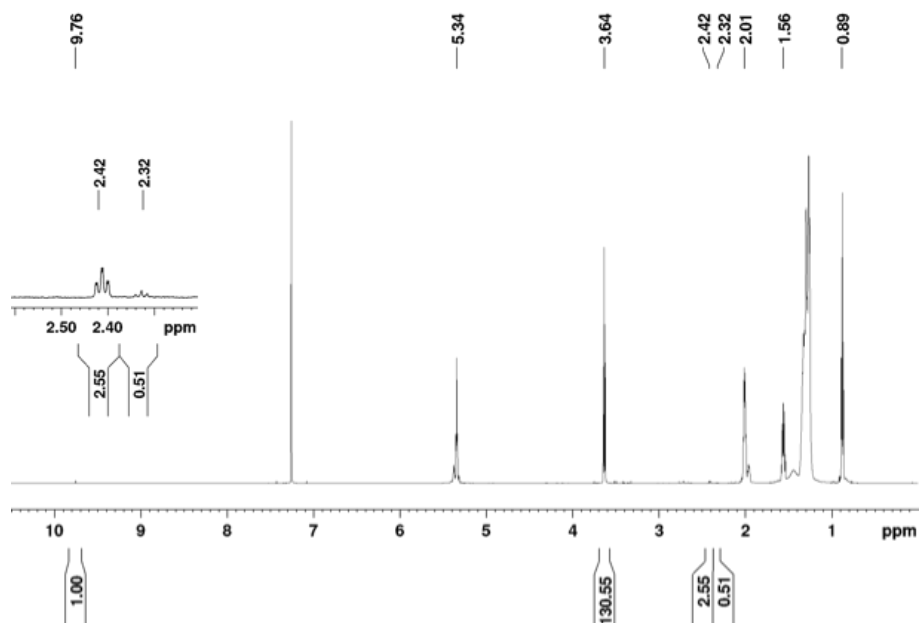


**Figure S17.**  $^1\text{H}$  NMR of the crude product oxidized from oleyl alcohol (C18-OH) (20 mM) by ACT (1 mM) in pH 10 buffer. Applied potential 0.8 V vs Ag/AgCl. Carbon felt 20 cm<sup>2</sup> as the working electrode, Pt wire 16 cm as the counter electrode, Ag/AgCl as the reference electrode, and temperature 25 °C.

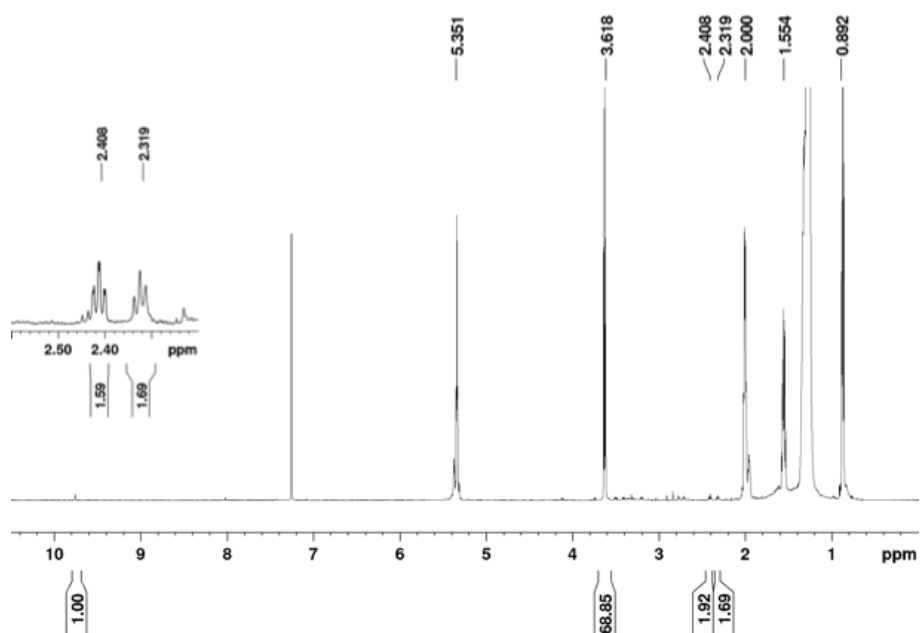


**Figure S18.**  $^1\text{H}$  NMR of the crude product oxidized from oleyl alcohol (C18-OH) (20 mM) by C10-NO· (1 mM) in pH 10 buffer. Applied potential 0.9 V vs Ag/AgCl. Carbon felt 20 cm<sup>2</sup> as the working electrode, Pt wire 16 cm as the counter electrode, Ag/AgCl as the reference electrode, and temperature 25 °C.

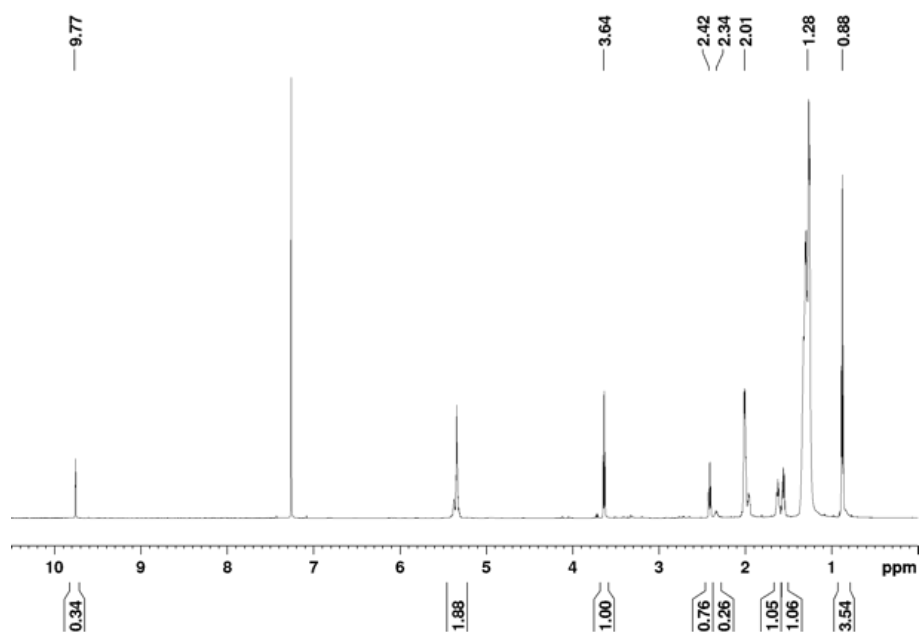


**Figure S19.**  $^1\text{H}$  NMR of the crude product oxidized from oleyl alcohol (C18-OH) (20 mM) by C14-NO $\cdot$  (1 mM) in pH 10 buffer. Applied potential 0.9 V vs Ag/AgCl. Carbon felt 20 cm $^2$  as the working electrode, Pt wire 16 cm as the counter electrode, Ag/AgCl as the reference electrode, and temperature 25  $^\circ\text{C}$ .

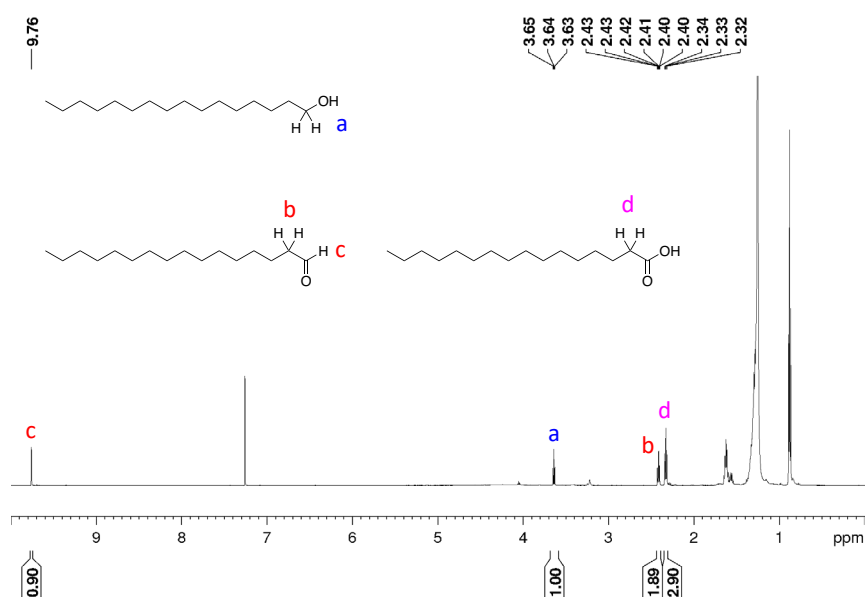


**Figure S20.**  $^1\text{H}$  NMR of the crude product oxidized from C16-OH (100 mM) by C14-NO $\cdot$  (5 mM) in pH 10 buffer. Applied potential 0.9 V vs Ag/AgCl. Carbon felt 20 cm $^2$  as the working electrode, Pt wire 16 cm as the counter electrode, Ag/AgCl as the reference electrode, and temperature 60  $^\circ\text{C}$  for 15 h.

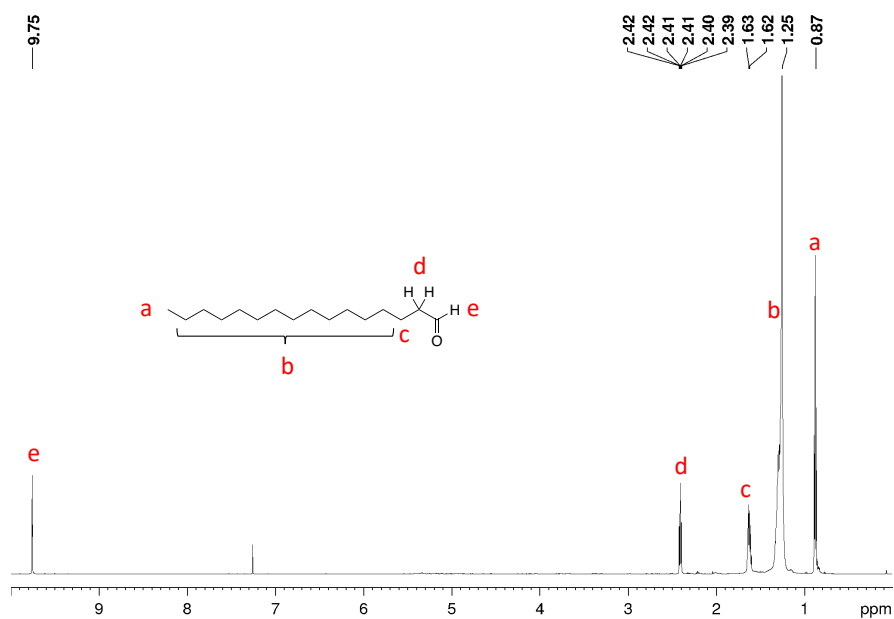


Figure S21. <sup>1</sup>H NMR of the purified hexadecanal (aldehyde from C16-OH) in CDCl<sub>3</sub>.

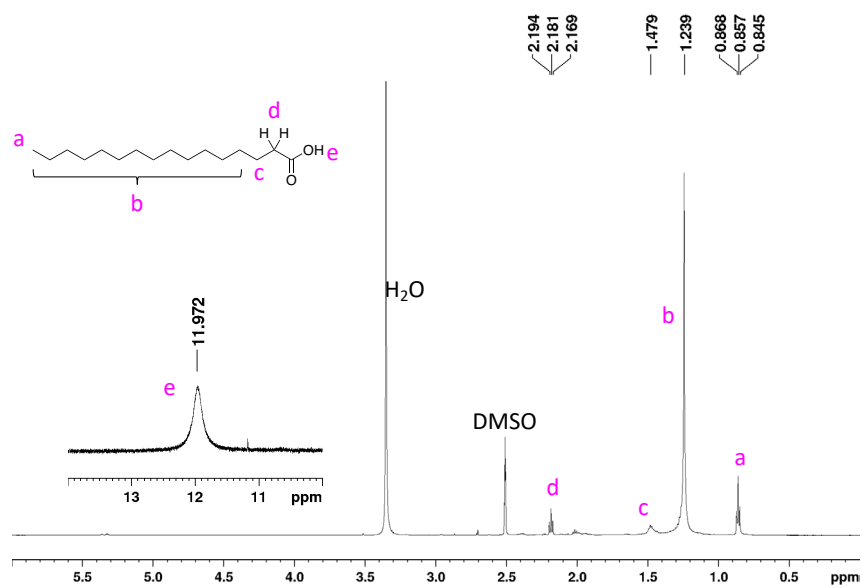


Figure S22. <sup>1</sup>H NMR of the purified hexadecanoic acid (carboxylic acid from C16-OH) in DMSO-*d*<sub>6</sub>.